NeuroImage 201 (2019) 116034

Contents lists available at ScienceDirect

NeuroImage

journal homepage: www.elsevier.com/locate/neuroimage

Role of the inhibitory system in shaping the BOLD fMRI response

Daniil P. Aksenov, Limin Li, Michael J. Miller, Alice M. Wyrwicz *

NorthShore University HealthSystem, Evanston, IL, 60201, USA

ARTICLE INFO

Keywords:
BOLD
fMRI
Time course
Visual
Somatosensory

ABSTRACT

The shape of the blood oxygenation level dependent (BOLD) functional magnetic resonance imaging (fMRI) signal can vary considerably even across structures of the same sensory pathway. Here, we characterized the temporal behavior of the stimulus-evoked BOLD response in the primary cortical and subcortical regions of the visual and somatosensory whisker systems in awake rabbits. Despite similar BOLD responses in the thalamic nuclei, considerable differences in shape and duration emerged between the sensory cortices. Whereas the BOLD response in the whisker barrel cortex (WBC) was non-adaptive, BOLD in the visual cortex (V1) showed adaptation similar to simultaneously-recorded LFP and single unit activity. Analysis of baseline neuronal activity revealed significantly lower firing rates in V1 vs. WBC. We hypothesized that these changes point to region-dependent differences in the inhibitory systems which shape the hemodynamic response in each structure. To test the effect of neuronal baseline level inhibition on the BOLD signal shape, we locally injected the $GABA_A$ agonist muscimol in WBC. Adaptation emerged in the BOLD response after injection, along with an overall decrease in baseline firing rate. These findings point to the importance of region-specific inhibitory shaping in determining the temporal behavior of the BOLD response in different brain areas.

1. Introduction

Functional magnetic resonance imaging (fMRI) relies upon blood oxygenation level dependent (BOLD) signal changes for mapping brain activation in humans and animals. It has been shown that the BOLD signal shape can vary across nodes within sensory pathways. In the visual system, Pawela et al. (2008) showed that temporal characteristics of BOLD signal in the primary and secondary visual cortex, superior colliculus, and thalamic nuclei were different in anesthetized rats, and that the BOLD time course was more transient in cortex than in subcortical visual structures. Similar findings were also reported in another visual study in anesthetized rats (Bailey et al., 2013). Studies of the somatosensory system in anesthetized rats also showed frequency-dependent differences in the shape and magnitude (Devonshire et al., 2012) of responses of cortical vs. subcortical regions during whisker stimulation. fMRI of the human auditory system revealed considerable differences in BOLD time courses among the cochlear nucleus, superior olivary complex, inferior colliculus, medial geniculate body, and auditory cortical areas (Sigalovsky and Melcher, 2006) during stimulation, with greater differences reported between cortical and subcortical structures. Such differences have also been reported in the auditory system of anesthetized rats (Cheung et al., 2012).

Comparing BOLD time course in different brain nodes, within a single sensory pathway as well as between sensory modalities, can provide information about the functional relationship between these nodes as well as the factors that shape the hemodynamic response. However, for relatively short stimulus durations, the differences among BOLD time courses within a sensory pathway can be very small. For example, the BOLD response in awake macaque monkeys (Baumann et al., 2010) with 8 s stimulation duration showed relatively little variation across cortical and subcortical nodes of the auditory system.

In order to characterize systematically the variation in BOLD response across different sensory structures, we compared the time courses of fMRI data acquired from both thalamic and cortical regions of the visual and somatosensory systems. These regions included the primary visual cortex (V1) and lateral geniculate nucleus (LGN), as well as the whisker barrel cortex (WBC) and ventral posteromedial nucleus (VPM). BOLD response was generated by using a long-duration sensory stimulation paradigm for each modality in order to capture both the initial and sustained behavior of the response. Experiments were performed in awake rabbits in order to avoid potential modulation of the BOLD signal by anesthesia.

Our findings reveal significant variation among the BOLD responses in the cortical and subcortical regions of the visual and somatosensory pathways. The temporal behavior of the BOLD signal was quite similar at

* Corresponding author. Center for Basic MR Research, NorthShore University HealthSystem, 1033 University Pl., Suite 100, Evanston, IL, 60201, USA.
E-mail address: a-wyrwicz@northwestern.edu (A.M. Wyrwicz).

https://doi.org/10.1016/j.neuroimage.2019.116034
Received 11 February 2019; Received in revised form 11 July 2019; Accepted 17 July 2019
Available online 19 July 2019

the thalamic level in the visual and somatosensory systems, but striking differences emerged in the cortex. The BOLD response in V1 exhibited a distinct initial peak followed by a decreased plateau, whereas the BOLD response in WBC showed no plateau phase following the initial peak. Moreover, analysis of the baseline activity in each region revealed a substantially lower rate of baseline neuronal firing in V1, suggesting an elevated level of baseline inhibition.

In order to examine the impact of increased baseline inhibition on the BOLD signal, we injected the $GABA_A$ agonist muscimol locally in WBC. This approach enabled us to enhance GABAergic activity locally while preserving thalamic inputs to the cortex. We hypothesized that modulating the inhibitory activity in WBC in this manner would decrease the baseline neuronal firing rate and produce a greater adaptation of the BOLD response during the sustained phase.

Our findings demonstrated that in the presence of muscimol the baseline single unit firing rate decreased in WBC and distinct adaptation emerged in the stimulus-evoked BOLD response. These results point to the role of inhibitory systems in shaping the hemodynamic response and highlight the importance of incorporating a more detailed picture of region-specific processes into the understanding of the factors that govern the hemodynamic response.

2. Methods

2.1. Animal Preparation

Female pigmented Dutch-belted rabbits (2–3 kg, 3–6 month of age) were used in these experiments, which were performed in accordance with the National Institutes of Health guidelines and NorthShore University HealthSystem Institutional Animal Care and Use Committee approved protocol.

Three groups of the animals were used for the experiments. In the first group BOLD fMRI responses to either visual (N = 12) or whisker (N = 11) stimulation were studied. In the second group neuronal responses to either visual (N = 4) or whisker (N = 4) stimulation were recorded. In the third group simultaneous BOLD fMRI, electrophysiology recording and localized brain microinjections of muscimol were conducted (N = 8). Total number of rabbits was 39.

Animals were anesthetized with a mixture of ketamine (50 mg/kg) and xylazine (10 mg/kg) and an incision was made in the scalp and the bone exposed on the top of the skull. A light-weight head restraining device containing four nylon bolts was implanted on top of the skull. This headbolt was used to secure the radiofrequency (RF) coil and the animal's head in the same position in order to obtain a constant imaging angle and slice positioning among subjects, as described previously (Wyrwicz et al., 2000). For neuronal recording the assembly consisting of a silica tube (Polymicro Technologies, Phoenix, AZ) containing a bundle of four 25 μm diameter gold-silver alloy microwires with formvar insulation (California Fine Wire, Grover Beach, CA) was implanted. The electrode materials were chosen, based on our previous evaluation, to minimize susceptibility artifacts in MR images. These electrodes terminated at different levels within a distance of 100 μm and were attached to a permanently implanted custom-made nylon microdrive that permitted vertical adjustments of its position. The microwires were connected to a small 6-pin connector that was embedded in dental acrylic. A 150 μm silver wire was placed between the skull and dura mater to serve as the reference electrode. A 200 μm silica injection cannula was attached to the microdrive. During implantation surgery, lambda was positioned 1.5 mm below bregma and the stereotaxic coordinates were as follows: anterior-posterior was 2 mm dorsal to bregma, medial-lateral was 6 mm from midline, and dorsal-ventral was under visual control for whisker barrel cortex and anterior-posterior was 7 mm dorsal to bregma, medial-lateral was 5.7 mm from midline, and dorsal-ventral was under visual control for visual cortex.

After a one week recovery from surgery, each subject was habituated to the imaging environment for 3–5 days prior to the experiments. For each experiment the rabbits were restrained by means of a cloth sleeve and secured in an acrylic imaging cradle by Velcro straps.

2.2. fMRI data collection and analysis

Imaging was performed using a Bruker (Billerica, MA) 9.4 T imaging spectrometer operating at a proton frequency of 400 MHz. This system was equipped with an Oxford horizontal magnet and an Acustar actively shielded gradient coil assembly with a clear bore of 15 cm. A flat, circular surface coil (20 mm in diameter) was used for RF transmission and reception. A multi-slice, single-shot gradient echo EPI pulse sequence, with a repetition time (TR) of 2 s and an echo time (TE) of 11 ms, was used to acquire images. Coronal images in a plane perpendicular to the surface coil were collected from eight contiguous slices (or four contiguous slices, in the case of muscimol experiments) 1.0 mm thickness, which included the electrode recording site, using an 80 × 80 matrix size and a 30 mm × 30 mm field of view (FOV), corresponding to an in-plane resolution of 375 μm × 375 μm. The slices were positioned to include V1 and LGN for visual stimulation experiments, and the WBC and VPM for vibrissae stimulation experiments. The rabbits received ten trials in each experiment, during which they were presented with the stimulation paradigm described below. The initial five images of each trial were discarded to ensure that the BOLD signal reached equilibrium. Anatomical images (512 × 512 matrix, 48 mm × 48 mm FOV, equivalent to 94 μm × 94 μm in-plane resolution) were also obtained using a multi-slice gradient echo sequence (1.0 mm slice thickness; TR, 1.5 s; TE, 20 ms, NA = 8). The fMRI data were registered using an affine method implemented in the ITK toolkit 14. Each trial was inspected for remaining head movement after registration, and any trials exhibiting movement were excluded from analysis. The remaining trials were averaged for each experiment. Activated voxels were detected using unsupervised support vector machine (SVM) analysis. Briefly, the mapping process is formulated as an outlier detection problem of one-class SVM that provides initial mapping results. These results are further refined by applying prototype selection and two-class SVM reclassification, as described previously (Song and Wyrwicz, 2009). Activated areas and time courses were then averaged across subjects and expressed as mean ± SEM.

2.3. Stimulus presentation

Whisker stimulation was delivered by a MRI-compatible system that incorporates real-time optical monitoring of the frequency and amplitude to ensure consistency of the vibration stimulus, as described previously (Li et al., 2012). We evaluated the BOLD response over a range of whisker stimulus frequencies (the results are shown in Supplementary Fig. S1). Based on these results a whisker stimulation frequency of 50 Hz with ± 0.3 mm deflection was used for all the experiments. B1, B2, and C1 whiskers on the left side were stimulated in each experiment. The visual stimulation consisted of a 2 × 2 array of green LEDs (16 lux output, delivered in a dark environment) flashing at 8 Hz delivered to the left eye. We previously evaluated the BOLD response produced by two different stimulation frequencies (Supplementary Fig. S2) and determined that an 8 Hz stimulation frequency produced an optimal BOLD response in the visual cortex of Dutch-Belted rabbits. The eyelids were held open using small tailor hooks during visual stimulation sessions. The stimulation paradigm consisted of a non-stimulus baseline period (15 images), a stimulation period (10 images) and a post-stimulus period (20 images) or for muscimol experiments: baseline period (25 images), a stimulation period (20 images) and a post-stimulus period (20 images).

2.4. Electrophysiological recording and microinjections

The electrophysiological signals from the microwires were fed through a miniature preamplifier to a multi-channel differential amplifier system (Neuralynx, Inc, USA). The signals were amplified, band-pass

filtered (300 Hz-3 kHz for single units and 1–150 Hz for LFP), and digitized (32 kHz/channel) using a Neuralynx data acquisition system. Electrophysiological signals from the neuronal activity were analyzed after removal of blocks of strong interference signals induced by gradient pulses. These blocks were detected by thresholding followed by one-dimensional mathematical morphology (Pratt, 1991) processing based on erosion and dilation functions. To capture the initial neuronal activity without interfering signals from the gradients, the stimulus onset was delayed for 150 ms from the MR acquisition triggering pulse. Subsequently, unit discrimination was performed offline using threshold detection followed by a cluster analysis of scatter plots of time and amplitude distances between the peak and valley of individual action potential wave shapes. The discriminated data were processed using Neuralynx and custom software written in Matlab and Visual Basic. Raster and peri-event histograms were constructed for each unit and experiment. Separate histograms were constructed for before and after injection of muscimol. In each histogram, the baseline firing rate and the magnitude of excitatory changes were computed. Baseline firing rate was calculated for all units. Mean single unit activity was calculated only for units exhibiting excitatory response. The mean of excitatory response always exceeded 1 SD of baseline after converting single unit activity to BOLD fMRI sampling frequency (0.5 Hz). Individual normalized cell histograms (spike frequency in Hz) were pooled together for each cell type and period of time to construct average population histograms. LFP signal energy was computed as the integral of the signal absolute value over non-overlapping time windows of 50 ms length outside the interference containing windows and averaged over ten trials for each experiment. The stimulation-related changes were calculated within the stimulation period for single units and LFP.

Muscimol (1.75 nmol/μl)) was dissolved in artificial cerebro-spinal fluid (ACSF) for injection. This concentration of muscimol was based on our preliminary studies which showed that under this concentration approximately 75–80% of neurons have firing frequency less than 1 Hz, corresponding to the neuronal firing frequency in V1. All injections (1 μl volume) were delivered through a silica tube/needle (190 μm OD and 100 μm ID, Polymicro Technologies, LLC, Phoenix, AZ) and connected to a Hamilton syringe using transparent Tygon tubing. Equal volumes of vehicle (ACSF) were injected in the same rabbits in randomized order (i.e., either before or after muscimol injection) following the same procedure in order to control for potential injection-related effects. Single units were monitored to ensure volume effect is minimized (Aksenov et al., 2014). Neuronal activity was recorded before, during and after (starting 15 min after the injection) pharmacological modulation. Based on our previous data (Aksenov et al., 2014), 15 min is sufficient to avoid any potential artifacts related to volume effect of the injection and to allow muscimol to diffuse throughout the whisker barrel cortex. The duration of the stimulation was extended for muscimol experiments in order to better capture the temporal behavior of the BOLD response.

2.5. Statistical analysis

The statistical analysis of parameters derived from the BOLD responses was conducted using one-way factorial ANOVA (Statistica, StatSoft, Tulsa, OK). ANOVA was followed by Tukey post-hoc analysis. The Spearman Rank Order correlation analysis was applied to indicate the strength and direction of a linear relationship between BOLD signals. Fisher z-transformation was used to establish the significance ($p < 0.05$) of the correlation coefficients. In order to compare the temporal responses of the BOLD and electrophysiological data in terms of their adaptation, initial and secondary phases were defined. The initial response was defined as a maximum during the first three time points of stimulation. The secondary response was defined as the maximum during last three points of the stimulation. Paired *t*-test was used to compare initial and secondary response magnitudes. The duration of BOLD response was defined as the time between the beginning of stimulation and time at which BOLD response returned to mean baseline + standard deviation of mean baseline. Due to the variation in the shape of the BOLD response, this parameter provided a more reliable measure of the response duration than full width at half maximum (FWHM). In the muscimol experiments, the post-stimulus undershoot was also analyzed statistically using paired *t*-test. Specifically, the minimal values as well as the total area 1 standard deviation below baseline were compared pre- and post-injection.

The electrophysiological data were converted to the BOLD sampling frequency (0.5 Hz) for comparison between these signals. One-way ANOVA was used to compare baselines in WBC and V1. Paired *t*-test was used to compare baselines, response magnitudes, and BOLD area before and after muscimol injection. Spearman Rank Order correlation analysis was used to calculate the strength and direction of a linear relationship between the BOLD signal and electrophysiological data during stimulation, between electrophysiological data or between BOLD responses in WBC. Fisher z-transformation was used to establish the significance of the correlation coefficients $p < 0.05$). The data are presented as mean ± SEM unless otherwise specified. In order to further analyze the significance of the changes produced in the BOLD temporal profiles by muscimol, 95% confidence intervals were used to plot the BOLD responses in the cortical and thalamic regions, as well as before and after muscimol and ACSF injection. Responses were normalized to the response mean in order to suppress individual variation in BOLD magnitude between animals (Supplementary Figs. S3 and S4).

3. Results

3.1. BOLD responses in cortical and subcortical structures

Examples of BOLD activation from single subjects during visual and whisker stimulation are shown in Fig. 1(a–d). As expected due to the crossing of the visual and somatosensory systems in the rabbit, all subjects showed a robust BOLD response contralateral to the stimulus presentation in the cortex as well as the thalamic nuclei, which form the primary excitatory inputs to the cortex. During visual stimulation (Fig. 1a and b), activation was present in V1 and LGN. In addition, we observed activation in the superior colliculi in an adjacent slice (not shown). During whisker stimulation, activation was detected in the WBC and VPM (Fig. 1c and d). In the cortex (Fig. 1e) visual and somatosensory stimulation produced strikingly different BOLD temporal responses. In V1 the BOLD response showed distinct transient and sustained components: an initial peak followed by a decreased plateau. In contrast, the BOLD time course in the whisker barrel cortex was non-adaptive during stimulation, without distinct peak and plateau features. Correlation analysis revealed no significant correlation between the BOLD responses in V1 and WBC. In the thalamic structures (Fig. 1f), however, the mean BOLD time courses averaged across subjects were quite similar for the visual and somatosensory systems. These responses in LGN and VPM were found to be strongly correlated ($r = 0.83$, $p < 0.01$).

Several parameters were defined to quantify and compare the variety of BOLD temporal responses in the cortical and subcortical regions of the visual and somatosensory systems. These parameters, which are summarized in Table 1, include initial and secondary response, defined as the peak magnitude during the first and last three time points of stimulation, respectively, as well as response duration.

The initial and secondary responses were compared using paired *t*-test to assess variation in the shape of the BOLD response within each region. As expected, no significant difference between initial and secondary response was found in WBC, whereas significant differences were found in V1 ($p = 0.000014$), LGN ($p = 0.047$) and VPM ($p = 0.015$). Correlation analysis was used to compare the shapes of the BOLD signal between cortical and subcortical structures for each sensory system. No significant positive correlation was found between the averaged BOLD time courses in V1 vs LGN and WBC vs VPM.

Analysis of mean BOLD durations in all regions using one-factor ANOVA showed significant main effect ($p = 0.016$, $F = 3.88$, $df = 3$).

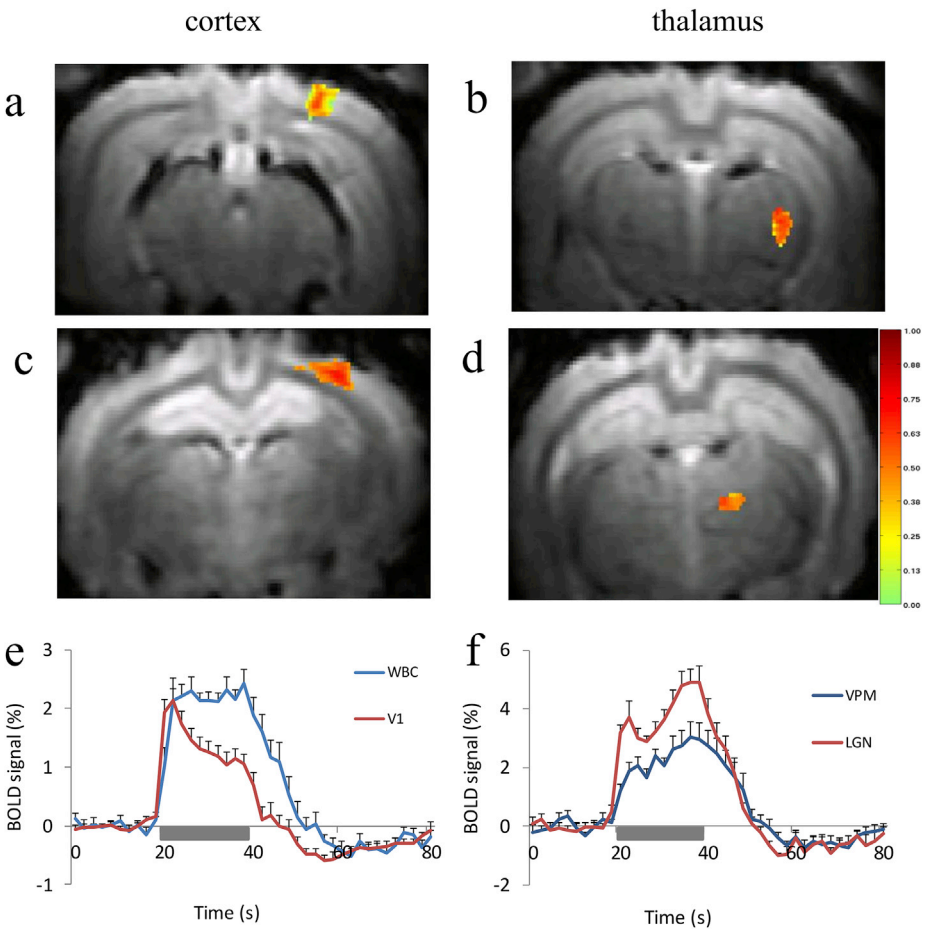

Fig. 1. Functional activation maps and BOLD temporal profiles in visual and somatosensory systems. Following visual stimulation, BOLD activation was observed in the primary visual cortex (a) and LGN (b). Vibrissae stimulation of three whiskers produced BOLD activation in the whisker barrel cortex (c) and VPM (d). Averaged temporal profiles were calculated for the cortical (e) and thalamic (f) regions. Note the well-correlated behavior of the BOLD responses in LGN and VPM, compared to the cortical regions. In contrast to WBC, the BOLD response in V1 shows significant adaptation. The gray bar indicates the timing of the stimulus presentation. The color bar indicates the probability of activation in each voxel.

Table 1
BOLD response parameters in cortical and thalamic structures.

	V1	LGN	WBC	VPM
Initial response (%)	2.28 ± 0.21[a]	3.99 ± 0.56	2.59 ± 0.26	2.24 ± 0.24
Secondary response (%)	1.21 ± 0.19	5.33 ± 0.55	2.53 ± 0.20	3.35 ± 0.53
Duration (s)	27.83 ± 1.31	32.00 ± 0.85	32.7 ± 1.40	31.78 ± 1.02

[a] Mean ± SEM.

Post hoc comparisons revealed that the BOLD duration in WBC was significantly longer than in V1 but the BOLD duration in VPM and LGN showed no significant difference.

3.2. Neuronal activity in WBC and V1

In order to compare neuronal activity in WBC and V1, LFP and single units were recorded in 8 rabbits (4 rabbits per group). A total of 49 and 44 single units were recorded in WBC and V1, respectively. As shown in Fig. 2, averaged LFP (Fig. 2a and b) and single unit (Fig. 2c and d) evoked responses in both cortices exhibited an initial peak followed by adaptation. The responses in V1 and WBC were strongly correlated ($r = 0.79$, $p < 0.01$ between LFP in WBC and V1; $r = 0.65$, $p < 0.05$ between SUs in WBC and V1).

In addition to the evoked neuronal responses, the baseline firing rates in V1 and WBC regions were also analyzed (Fig. 3). The mean baseline activity in WBC (Fig. 3a) was found to be 3.3 ± 1.03 spikes/s whereas in V1 it was 0.52 ± 0.09 spikes/s. One-factor ANOVA showed significant main effect for region factor ($p < 0.002$, $F = 10.7$, $df = 1$). The distributions of baseline firing rates in both regions were further analyzed and are shown in Fig. 3b and c. The dominant activity in V1 was under 1 spikes/s (82% of cells), whereas in WBC only 50% of cells showed baseline activity under 1 spikes/s, and 20% of cells had a baseline firing rate of more than 3 spikes/s.

3.3. Effect of muscimol on BOLD fMRI and neuronal activity

In order to test the hypothesis that the difference in baseline neuronal activity and BOLD response adaptation in WBC and V1 is due to a lower baseline level of inhibition in WBC, the $GABA_A$ agonist muscimol was locally injected into WBC and simultaneous BOLD fMRI and electrophysiology recording were performed before and after injection.

As illustrated in Fig. 4, muscimol decreased the area of the cortical BOLD response to 56.8 ± 6.0% of the initial level ($p < 0.004$) (Fig. 4a and b) by increasing intracortical GABA-ergic inhibition. ACSF injection did not produce a significant change in the BOLD area (data shown in the Supplementary Figs. S6–8). The mean BOLD response magnitude decreased to 74.2 ± 6.7% of pre-injection level ($p < 0.005$) (Fig. 4c and d). In contrast, adaptation emerged in the secondary phase of the response, which decreased significantly to 68.6 ± 9.2% of initial level ($p < 0.03$). The correlation between the BOLD responses before and after muscimol injection became non-significant. ACSF injection did not produce significant changes either in mean or maximum BOLD response magnitude. In order to rule out that the change in BOLD response shape under muscimol was merely a consequence of the difference in activated area, we compared BOLD responses before injection from two regions of interest (ROIs): the entire activated region in WBC, and a ROI equivalent to the post-injection BOLD (Supplementary Fig. S5). There was no difference in the shape of the BOLD signal between these regions, as

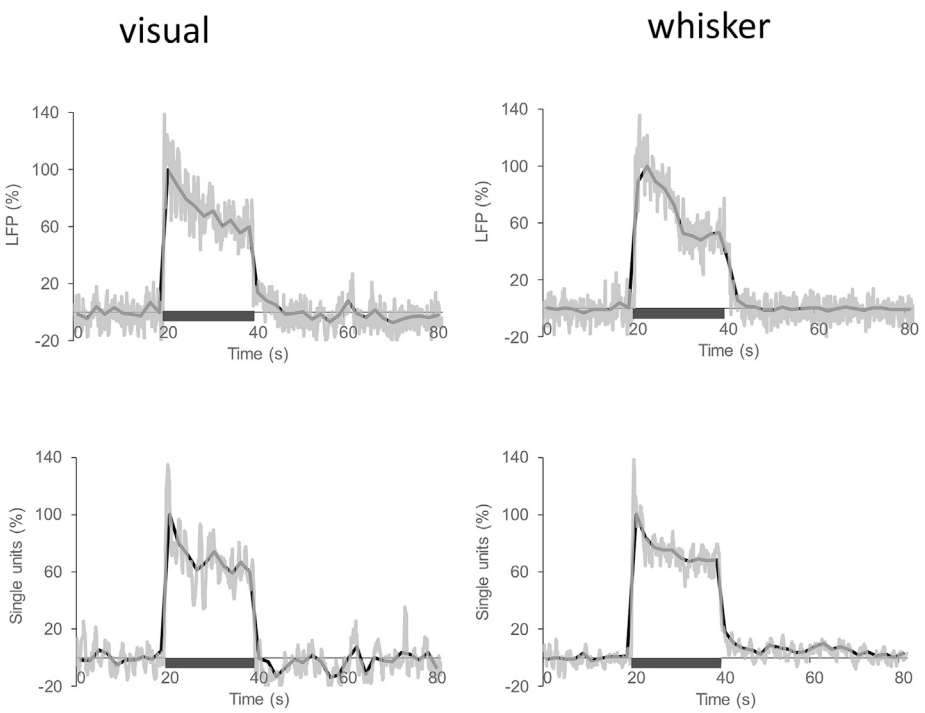

Fig. 2. Stimulus-evoked neuronal activity in the visual and somatosensory cortices. LFP (a,b) and single unit (c,d) responses were recorded from layer IV of either WBC or V1 during vibrissae or visual stimulation, respectively. All responses exhibited distinct transient and sustained (i.e., peak and plateau) features and were well correlated between the two cortices. Averaged responses are shown using both 100 ms (gray) and 1 s (black) bins. The gray bar on the horizontal axis shows the timing of the stimulus presentation.

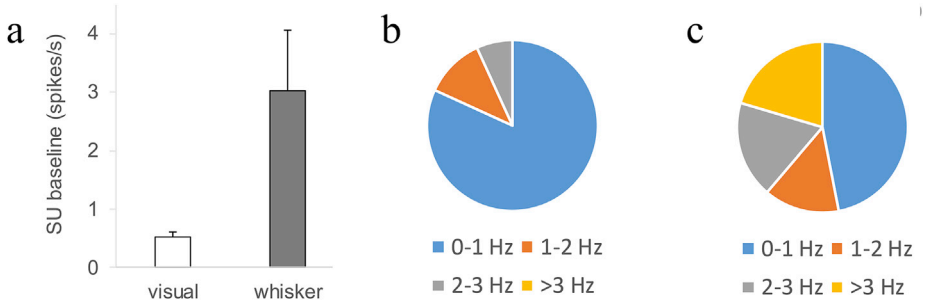

Fig. 3. Baseline single unit firing in the visual and somatosensory cortices. The mean baseline firing rate was significantly greater in WBC than in V1 (a). This difference is reflected in the distribution of baseline firing rates recorded in V1 (b) (n = 44) and WBC (c) (n = 49). Note the greater proportion of cells with a higher firing rate, particularly > 3 Hz, in WBC. The error bars indicate the SEM.

indicated by the correlation coefficient ($r = 0.83$, $p < 0.01$). The magnitude of the BOLD response from the smaller ROI was 19% higher ($p < 0.002$), as would be expected from a sub-region more closely localized to the principal site of activation. The duration of the BOLD response was 51.3 ± 1.5s before and 46.3 ± 1.4s after muscimol injection ($p < 0.026$). For comparison, the duration of BOLD response was 50.8 ± 1.1s before and 50.4 ± 1.0s after ASCF injection. No statistically significant differences were found in the post-stimulus baseline undershoot of the BOLD reseponse before vs. after muscimol injection. The LFP evoked response (Fig. 4e and f) decreased to 90.7% of the pre-injection level ($p < 0.029$) after muscimol injection, and the single unit evoked response decreased to 47.5% of preinjection level ($p < 0.017$).

The effects of muscimol on the baseline neuronal activity in WBC are shown in Fig. 5. A total of 89 single units were recorded. The mean baseline level of single unit firing (Fig. 5a) was 2.95 ± 0.5 spikes/s before injection and significantly decreased ($p < 0.0002$) to 0.97 ± 0.2 after injection, which represents 33% of the pre-injection level. Paired *t*-test showed that the LFP baseline (Fig. 5b) decreased to 92.3 ± 2.2% of the pre-injection level following muscimol injection ($p < 0.009$). The proportion of cells with a firing rate under 1 spikes/s increased from 40% before injection to 76% after injection (Fig. 5c and d). The proportion of cells with activity >3 spikes/s decreased from 25% before injection to 9% after injection.

Muscimol did not significantly affect BOLD response in the thalamus (Fig. 6). Similar BOLD response to whisker stimulation was observed in VPM before and after muscimol injection (Fig. 6a and b). The averaged temporal profiles of the BOLD response in VPM are shown in Fig. 6c and d. The mean response magnitude was 2.37 ± 0.2% before injection and 2.09 ± 0.2% after injection. The duration of the response was 50.29 ± 3.0s before injection and 50.56 ± 3.6s after injection. The correlation coefficient of the responses before and after injection was 0.7 ($p < 0.001$).

4. Discussion

Our results show that the characteristics of the BOLD evoked response can vary considerably between the primary sensory cortices. During simple visual or whisker stimulation, the BOLD responses in the LGN and VPM correlated well with one another, whereas the responses in WBC and V1 showed significant differences in shape and duration. The LGN and VPM are quite similar in their organization, which likely accounts for the consistency in their BOLD responses. Input to these structures includes the main excitatory input from the retina (LGN) or trigeminal nucleus (VPM), corticothalamic feedback, as well as inhibitory input

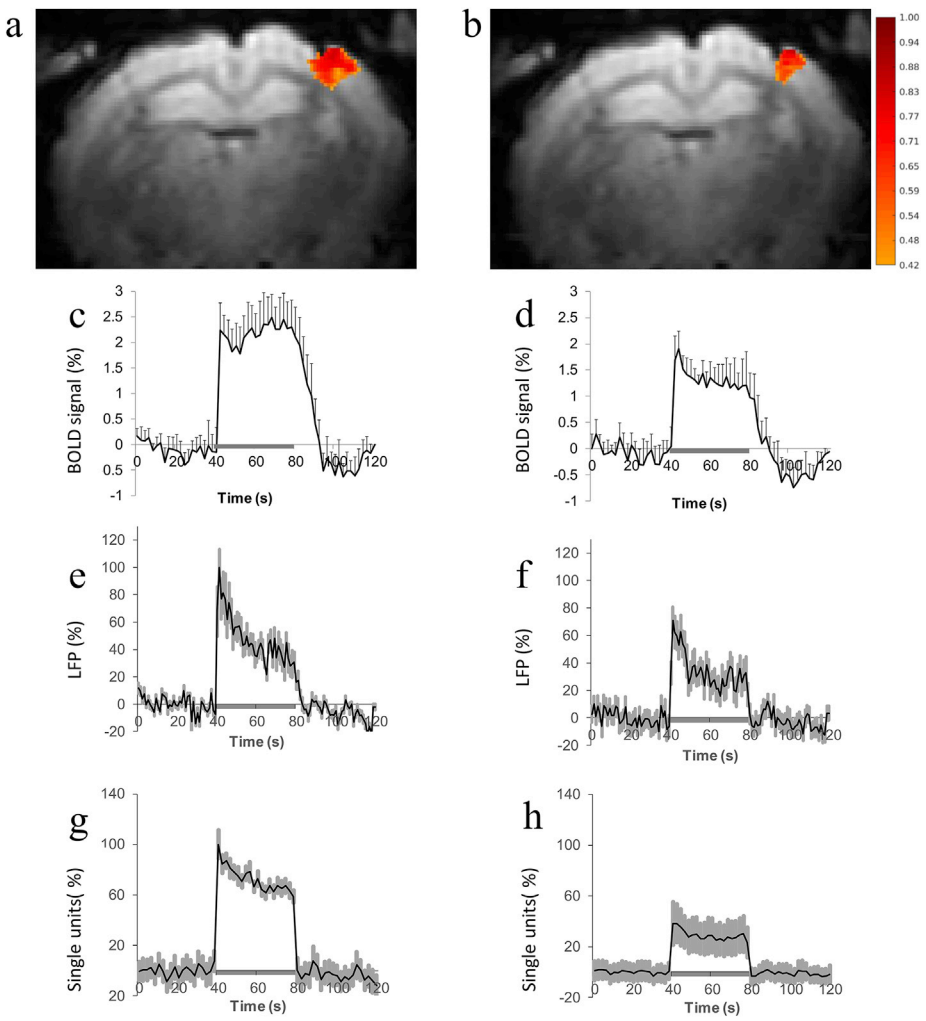

Fig. 4. Effect of muscimol on stimulus-evoked BOLD and neuronal responses. Before muscimol injection (a) a robust BOLD response was observed which extended through the depth of the cortex. The activated area decreased under muscimol (b). The averaged temporal profile from a region corresponding to the post-injection area exhibited a non-adaptive temporal profile before injection (c). Distinct adaptation emerged in the BOLD response under the effect of muscimol (d). While the maximum magnitude of the BOLD response remained unchanged, the mean magnitude decreased under muscimol. Before injection, both LFP (e) and single units (f) had similar peak and plateau shapes which were maintained under muscimol (g,h), although the level of baseline and stimulus-evoked activity decreased. The gray bars indicate the timing of the stimulus presentation. The color bar indicates the probability of activation in each voxel.

from the thalamic reticular nucleus. In terms of their architecture, the LGN and VPM have approximately the same density of relay cells, but the density of interneurons is higher in LGN (Cavdar et al., 2014). The difference in response magnitude between the LGN and VPM likely reflects differences between the two stimulation modalities. However, the high correlation of the BOLD temporal responses in LGN and VPM suggests that they receive and process information in a similar way.

Based on the high correlation of the thalamic BOLD responses, which constitute the main input to the primary sensory cortices, V1 and WBC might also be expected to show similar behavior in terms of the shape and duration of the BOLD response. However, whereas evoked responses in both cortical regions reached the same magnitude of initial response, V1 exhibited a decreased plateau phase following the initial peak, which was not present in WBC. Furthermore, the duration of the evoked BOLD response was significantly shorter in V1 than in WBC or the thalamic nuclei. It is unlikely that the longer BOLD response in WBC merely reflects the difference in secondary response magnitude, as the temporal behavior of the responses in LGN and VPM was quite similar despite a difference in magnitude. Of course, it is difficult to ensure complete equivalence of stimuli across different sensory modalities. The visual and whisker systems respond differently to stimulation frequency, and thus, as described in the Methods, the frequency and magnitude of the stimulus presentation were chosen so as to produce the optimal BOLD response in each region. While we cannot rule out the possibility some of the variation between V1 and WBC may be related to the stimulus frequency, the similarity of the BOLD responses in VPM and LGN, as described above, indicate that the differences were not substantial at the level of the thalamus. The nature of these differences in temporal behavior should therefore correspond to the particular vascular and neuronal processes that generate the hemodynamic response in each cortical region.

It is unlikely that intrinsic vascular differences alone account for the difference in response adaptation that we observed in these structures. While it has been shown that regional variations in brain capillary density (Cavaglia et al., 2001) exist, they were found mostly between hippocampal regions. Wu at al (Wu et al., 2014). performed a direct comparison between microvasculature in the whisker barrel and visual cortices in mice and reported some differences in vascular density that were restricted to specific layers. Increased microvascular density has been associated with greater resting-state metabolic demand (Cavaglia et al., 2001; Malonek et al., 1997; Weber et al., 2008) and greater responsivity of neurons to functional tasks (Harrison et al., 2002), and thus the vascularization in cortical regions is to some degree a static reflection of local differences in overall neuronal activity. However, the significant variation in temporal behavior that we observed in cortical BOLD responses, despite similar thalamic inputs, raises the question of how neuronal activity, via the interaction of neurons with the vasculature, dynamically shapes the BOLD signal in each region.

Cortical BOLD is believed to reflect primarily postsynaptic potentials originating from thalamocortical inputs as well as intracortical processing, which further spreads and modifies the input across layers and between columns. Postsynaptic potentials correspond to the activity of excitatory (i.e., glutamatergic) and inhibitory (i.e., GABAergic) synapses, which produce a hemodynamic response, and thus a change in the BOLD signal, through distinct mechanisms (Logothetis and Pfeuffer, 2004). A

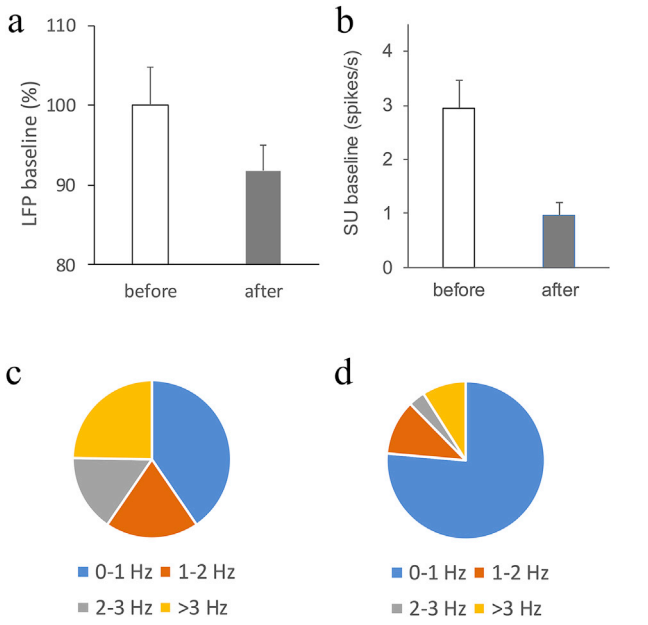

Fig. 5. Effect of muscimol on baseline neuronal activity. The mean baseline LFP (a) and single unit activity (b) both significantly decreased after muscimol injection in WBC. The distribution of baseline firing rates in WBC is shown before (c) and after (d) local muscimol injection. Note the increase in the proportion of cells with firing rates of 0–1 Hz under muscimol.

number of possible mechanisms have been proposed for the control of cerebral blood flow response via glutamatergic excitation, including nitric oxide (NO), the vasoactive metabolites of arachidonic acid (AA), and K^+ (Attwell et al., 2010; Nippert et al., 2017). In contrast, the hemodynamic impact of inhibitory systems can occur through direct interaction with $GABA_A$ receptors on blood vessels (Vaucher et al., 2000) in addition to their action upon excitatory cells. An underlying difference in the excitatory and inhibitory systems in these regions could thus lead to a difference in the temporal dynamics of the BOLD response, including changes in response adaptation.

Although the excitatory architecture in the visual and somatosensory cortices is quite similar, it has been shown previously that translaminar inhibition by interneurons is more prominent in V1 than in WBC (Katzel et al., 2011). This mechanism probably ensures increased specificity to stimuli in the columns of the visual cortex by limiting spreading of the excitation, in contrast to the barrels in the somatosensory cortex where spreading of neuronal activity through trans-columnar processing is more extensive (Feldmeyer et al., 2013). The enhanced inhibitory environment in V1, as reflected in the lower baseline neuronal firing rate that we observed in this region, could therefore produce a more rapid decay of the BOLD signal via a greater impact of GABA upon the local vasculature. Previous studies have established that translaminar inhibition plays a crucial role in controlling the magnitude of neuronal activity (Olsen et al., 2012) and that the BOLD signal may depend on interneuron function (Angenstein, 2014).

Our electrophysiological data showed that the stimulus-evoked neuronal responses more closely resembled the BOLD response in V1 than in WBC. Moreover, analysis of the average baseline (i.e., spontaneous) neuronal activity revealed a much lower level of activity in V1 than in WBC. Based on these findings, we sought to test the dependence of the BOLD signal shape on the level of baseline inhibition, as opposed to evoked neuronal response. We hypothesized that increasing the local level of baseline inhibition using the $GABA_A$ agonist muscimol would elicit in the WBC a BOLD response to stimulation that more closely resembled that in V1, with a distinct peak followed by a plateau. As expected, neuronal activity exhibited a significant decrease in both baseline and evoked response magnitude after muscimol injection. Averaged LFP and single unit activity maintained their peak and plateau shape, as observed previously, which confirms that muscimol inhibited neuronal activity without substantially changing the adaptation of these responses. However, the BOLD response in WBC developed distinct peak and plateau features that were not present before muscimol injection.

Although the mechanisms that drive such adaptation of the BOLD response are not entirely known, they likely reflect a complex interplay among both neuronal and vascular effects. From a neuronal perspective, the BOLD response in the cortex is the product of two main contributions: excitatory thalamocortical input and intracortical processing of this input as it spreads within and between columns, which is modulated by inhibitory shaping. An increase in baseline inhibition decreases excitatory activity associated with intracortical processing. Notably, the BOLD

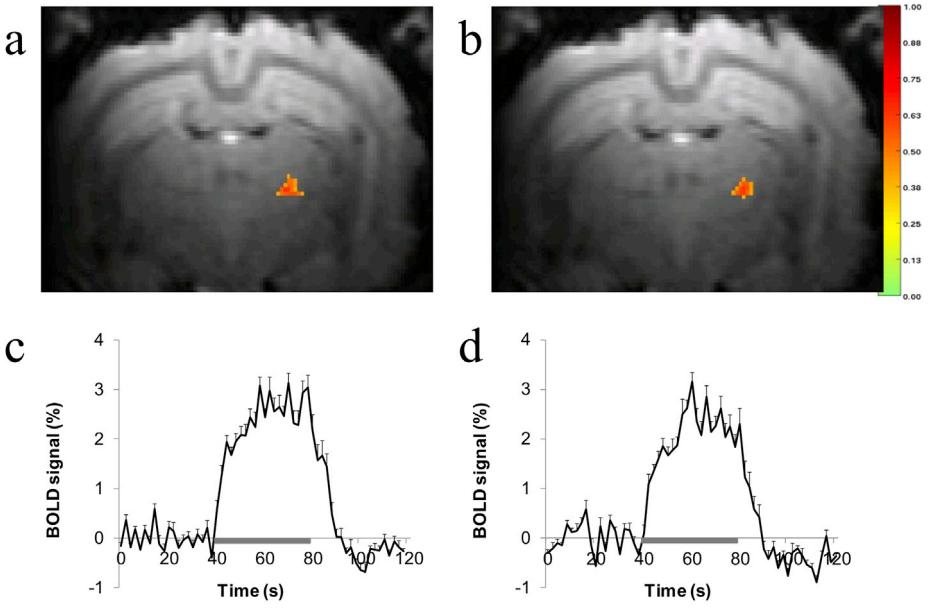

Fig. 6. Effect of muscimol on BOLD response in the thalamus. Similar BOLD activation was present during whisker stimulation in VPM before (a) and after (b) localized injection of muscimol. The averaged temporal behavior of the BOLD response in this region was quite similar in magnitude and duration before (c) and after (d) injection. The gray bars indicate the timing of the stimulus presentation. The color bar indicates the probability of activation in each voxel.

response in the thalamus was the same before and after muscimol injection in terms of area, magnitude, shape and duration (Fig. 6), indicating that the thalamocortical input did not substantially change. This finding is in agreement with Fox et al. (2003) who demonstrated via direct recording of neuronal activity from VPM that thalamic input to the cortex was not affected during cortical application of muscimol.

In terms of the vasculature, the hemodynamic response to stimulation involves dilation of capillaries, arterioles and arteries via propagated vasodilation initiated by the neuronal trigger. Like the neuronal response to stimulation, the dynamics of the vascular response are also complex. Longer duration stimuli show a peak and plateau response pattern, which has been observed using optical methods as well as in the BOLD response. This pattern has been ascribed to the behavior of the more distant pial arteries, which tend to return to the baseline after the initial peak, whereas the plateau phase is localized to the central region where the response is more sustained. The amplitude of the plateau has been reported to be more variable than the initial peak, which is also the case for the BOLD response (Hillman, 2014). The venous component which contributes significantly to the BOLD response has somewhat different temporal behavior, with venules draining the blood with a delayed passive dilation and longer lag than arteries (He et al., 2018). Thus, it is possible that the secondary phase of the BOLD response reflects a greater contribution from venous effects. Increased baseline inhibition may change the baseline relationship between the arterial and venous components by direct action upon vessels as well as via decreased neuronal firing, leading to a change in the BOLD response shape.

Dissociation between the temporal behavior of the BOLD signal and neuronal activity has been shown in many previous studies, including our own (Aksenov et al., 2014, 2015; Kim et al., 2004; Logothetis et al., 2001; Rauch et al., 2008). It is believed that synaptic depression as well as cell intrinsic and inhibitory mechanisms may be the sources of neuronal response adaptation (Kohn, 2007). A variety of models have attempted to describe the transfer of the underlying neuronal activity into the shape of the hemodynamic function (Buxton, 2012; Buxton et al., 2004). Our findings here suggest that the temporal behavior of the BOLD response to stimulation can be modulated significantly by the level of neuronal baseline inhibition and does not necessarily correspond to the shape of the neuronal evoked response. Neuronal baseline inhibition, as indicated by baseline levels of GABA measured with MRS, was previously shown to be inversely correlated with the magnitude of BOLD response (Chen et al., 2005; Kurcyus et al., 2018) but its relationship to the temporal behavior of the response was not examined.

In conclusion, the activity within the cortex that drives the BOLD response involves a complex interplay between neuronal excitation and inhibition as well as the local vasculature. The underlying processes are not entirely understood, but our findings here indicate that regional variations in BOLD temporal behavior depend on the local level of baseline inhibition. The differences in the distribution of baseline neuronal firing rates measured between the sensory cortices point to the role of intracortical inhibition in generating the BOLD response shape. Indeed, we were able to induce BOLD adaptation by locally increasing the GABAergic inhibition via muscimol injection. These effects could vary substantially from region to region in the cortex as well as subcortical structures, and further work is necessary to unravel the specific mechanisms of interaction between excitatory/inhibitory systems as well as the vasculature.

Acknowledgements

This work was supported in part by National Institute of Neurological Disorders and Stroke, United States [grant number R01NS107383 to DPA].

Appendix A. Supplementary data

Supplementary data to this article can be found online at https://doi.org/10.1016/j.neuroimage.2019.116034.

References

Aksenov, D.P., Li, L., Iordanescu, G., Miller, M.J., Wyrwicz, A.M., 2014. Volume effect of localized injection in functional MRI and electrophysiology. Magn. Reson. Med. 72, 1170–1175. https://doi.org/10.1002/mrm.24996.

Aksenov, D.P., Li, L., Miller, M.J., Iordanescu, G., Wyrwicz, A.M., 2015. Effects of anesthesia on BOLD signal and neuronal activity in the somatosensory cortex. J. Cereb. Blood Flow Metab. 35, 1819–1826. https://doi.org/10.1038/jcbfm.2015.130.

Angenstein, F., 2014. The actual intrinsic excitability of granular cells determines the ruling neurovascular coupling mechanism in the rat dentate gyrus. J. Neurosci. 34, 8529–8545. https://doi.org/10.1523/JNEUROSCI.0472-14.2014.

Attwell, D., Buchan, A.M., Charpak, S., Lauritzen, M., Macvicar, B.A., Newman, E.A., 2010. Glial and neuronal control of brain blood flow. Nature 468, 232–243. https://doi.org/10.1038/nature09613.

Bailey, C.J., Sanganahalli, B.G., Herman, P., Blumenfeld, H., Gjedde, A., Hyder, F., 2013. Analysis of time and space invariance of BOLD responses in the rat visual system. Cerebr. Cortex 23, 210–222. https://doi.org/10.1093/cercor/bhs008.

Baumann, S., Griffiths, T.D., Rees, A., Hunter, D., Sun, L., Thiele, A., 2010. Characterisation of the BOLD response time course at different levels of the auditory pathway in non-human primates. Neuroimage 50, 1099–1108. https://doi.org/10.1016/j.neuroimage.2009.12.103.

Buxton, R.B., 2012. Dynamic models of BOLD contrast. Neuroimage 62, 953–961. https://doi.org/10.1016/j.neuroimage.2012.01.012.

Buxton, R.B., Uludag, K., Dubowitz, D.J., Liu, T.T., 2004. Modeling the hemodynamic response to brain activation. Neuroimage 23 (Suppl. 1), S220–S233.

Cavaglia, M., Dombrowski, S.M., Drazba, J., Vasanji, A., Bokesch, P.M., Janigro, D., 2001. Regional variation in brain capillary density and vascular response to ischemia. Brain Res. 910, 81–93.

Cavdar, S., Bay, H.H., Yildiz, S.D., Akakin, D., Sirvanci, S., Onat, F., 2014. Comparison of numbers of interneurons in three thalamic nuclei of normal and epileptic rats. Neurosci Bull 30, 451–460. https://doi.org/10.1007/s12264-013-1402-3.

Chen, Z., Silva, A.C., Yang, J., Shen, J., 2005. Elevated endogenous GABA level correlates with decreased fMRI signals in the rat brain during acute inhibition of GABA transaminase. J. Neurosci. Res. 79, 383–391.

Cheung, M.M., Lau, C., Zhou, I.Y., Chan, K.C., Cheng, J.S., Zhang, J.W., Ho, L.C., Wu, E.X., 2012. BOLD fMRI investigation of the rat auditory pathway and tonotopic organization. Neuroimage 60, 1205–1211. https://doi.org/10.1016/j.neuroimage.2012.01.087.

Devonshire, I.M., Papadakis, N.G., Port, M., Berwick, J., Kennerley, A.J., Mayhew, J.E., Overton, P.G., 2012. Neurovascular coupling is brain region-dependent. Neuroimage 59, 1997–2006.

Feldmeyer, D., Brecht, M., Helmchen, F., Petersen, C.C., Poulet, J.F., Staiger, J.F., Luhmann, H.J., Schwarz, C., 2013. Barrel cortex function. Prog. Neurobiol. 103, 3–27. https://doi.org/10.1016/j.pneurobio.2012.11.002.

Fox, K., Wright, N., Wallace, H., Glazewski, S., 2003. The origin of cortical surround receptive fields studied in the barrel cortex. J. Neurosci. 23, 8380–8391.

Harrison, R.V., Harel, N., Panesar, J., Mount, R.J., 2002. Blood capillary distribution correlates with hemodynamic-based functional imaging in cerebral cortex. Cerebr. Cortex 12, 225–233.

He, Y., Wang, M., Chen, X., Pohmann, R., Polimeni, J.R., Scheffler, K., Rosen, B.R., Kleinfeld, D., Yu, X., 2018. Ultra-slow single-vessel BOLD and CBV-based fMRI spatiotemporal dynamics and their correlation with neuronal intracellular calcium signals. Neuron 97, 925–939 e925. https://doi.org/10.1016/j.neuron.2018.01.025.

Hillman, E.M., 2014. Coupling mechanism and significance of the BOLD signal: a status report. Annu. Rev. Neurosci. 37, 161–181. https://doi.org/10.1146/annurev-neuro-071013-014111.

Katzel, D., Zemelman, B.V., Buetfering, C., Wolfel, M., Miesenbock, G., 2011. The columnar and laminar organization of inhibitory connections to neocortical excitatory cells. Nat. Neurosci. 14, 100–107. https://doi.org/10.1038/nn.2687.

Kim, D.S., Ronen, I., Olman, C., Kim, S.G., Ugurbil, K., Toth, L.J., 2004. Spatial relationship between neuronal activity and BOLD functional MRI. Neuroimage 21, 876–885.

Kohn, A., 2007. Visual adaptation: physiology, mechanisms, and functional benefits. J. Neurophysiol. 97, 3155–3164. https://doi.org/10.1152/jn.00086.2007.

Kurcyus, K., Annac, E., Hanning, N.M., Harris, A.D., Oeltzschner, G., Edden, R., Riedl, V., 2018. Opposite dynamics of GABA and glutamate levels in the occipital cortex during visual processing. J. Neurosci. 38, 9967–9976. https://doi.org/10.1523/JNEUROSCI.1214-18.2018.

Li, L., Weiss, C., Talk, A.C., Disterhoft, J.F., Wyrwicz, A.M., 2012. A MRI-compatible system for whisker stimulation. J. Neurosci. Methods 205, 305–311.

Logothetis, N., Pauls, J., Augath, M., Trinath, T., Oeltermann, A., 2001. Neurophysiological investigation of the basis of the fMRI signal. Nature 412, 150–157.

Logothetis, N.K., Pfeuffer, J., 2004. On the nature of the BOLD fMRI contrast mechanism. Magn. Reson. Imaging 22, 1517–1531. https://doi.org/10.1016/j.mri.2004.10.018.

Malonek, D., Dirnagl, U., Lindauer, U., Yamada, K., Kanno, I., 1997. Vascular imprints of neuronal activity: relationships between the dynamics of cortical blood flow, oxygenation, and volume changes following sensory stimulation. Proc. Natl. Acad. Sci. U.S.A. 94, 14826–14831.

Nippert, A.R., Biesecker, K.R., Newman, E.A., 2017. Mechanisms mediating functional hyperemia in the brain. The Neuroscientist, 1073858417703033. https://doi.org/10.1177/1073858417703033.

Olsen, S.R., Bortone, D.S., Adesnik, H., Scanziani, M., 2012. Gain control by layer six in cortical circuits of vision. Nature 483, 47–52. https://doi.org/10.1038/nature10835.

Pawela, C.P., Hudetz, A.G., Ward, B.D., Schulte, M.L., Li, R., Kao, D.S., Mauck, M.C., Cho, Y.R., Neitz, J., Hyde, J.S., 2008. Modeling of region-specific fMRI BOLD neurovascular response functions in rat brain reveals residual differences that correlate with the differences in regional evoked potentials. Neuroimage 41, 525–534. https://doi.org/10.1016/j.neuroimage.2008.02.022.

Pratt, W., 1991. Morphological Image Processing, second ed. Wiley-Interscience, New York.

Rauch, A., Rainer, G., Logothetis, N.K., 2008. The effect of a serotonin-induced dissociation between spiking and perisynaptic activity on BOLD functional MRI. Proc. Natl. Acad. Sci. U. S. A. 105, 6759–6764.

Sigalovsky, I.S., Melcher, J.R., 2006. Effects of sound level on fMRI activation in human brainstem, thalamic and cortical centers. Hear. Res. 215, 67–76. https://doi.org/10.1016/j.heares.2006.03.002.

Song, X., Wyrwicz, A.M., 2009. Unsupervised spatiotemporal fMRI data analysis using support vector machines. Neuroimage 47, 204–212. https://doi.org/10.1016/j.neuroimage.2009.03.054.

Vaucher, E., Tong, X.K., Cholet, N., Lantin, S., Hamel, E., 2000. GABA neurons provide a rich input to microvessels but not nitric oxide neurons in the rat cerebral cortex: a means for direct regulation of local cerebral blood flow. J. Comp. Neurol. 421, 161–171.

Weber, B., Keller, A.L., Reichold, J., Logothetis, N.K., 2008. The microvascular system of the striate and extrastriate visual cortex of the macaque. Cerebr. Cortex 18, 2318–2330. https://doi.org/10.1093/cercor/bhm259.

Wu, J., He, Y., Yang, Z., Guo, C., Luo, Q., Zhou, W., Chen, S., Li, A., Xiong, B., Jiang, T., Gong, H., 2014. 3D BrainCV: simultaneous visualization and analysis of cells and capillaries in a whole mouse brain with one-micron voxel resolution. Neuroimage 87, 199–208. https://doi.org/10.1016/j.neuroimage.2013.10.036.

Wyrwicz, A.M., Chen, N.-K., Li, L., Weiss, C., Disterhoft, J.F., 2000. fMRI of visual system activation in the conscious rabbit. Magn. Reson. Med. 44, 474–478.